

Article

# Geochemical Behavior of Potentially Toxic Elements in Riverbank-Deposited Weathered Tailings and Their Environmental Effects: Weathering of Pyrite and Manganese Pyroxene

Yeongkyoo Kim

School of Earth System Sciences, Kyungpook National University, Daegu 41566, Korea; ygkim@knu.ac.kr; Tel.: +82-53-950-5360

Received: 26 March 2020; Accepted: 2 May 2020; Published: 7 May 2020



**Abstract:** Uncontrolled management of mine tailings can cause serious environmental problems. Red and black deposits of weathered mine tailings are observed in the upstream of the Nakdong River in Korea, washed away from abandoned mines during floods. Herein, the geochemical and mineralogical changes that occur during weathering of these deposited mine tailings and the mobility of resulting potentially toxic elements were investigated. Primarily, johansennite (manganese pyroxene) was identified in the deposits. Goethite and jarosite were identified as secondary minerals in the red or brown layers. Manganese oxide (MnO) formed by the weathering of johansennite in the black layers and schwertmannite in the red and brown layers were also identified via energy-dispersive X-ray spectroscopy. The three most abundant potentially toxic elements in the residual and iron and manganese oxide fractions were Zn, Pb and As. The high percentage of potentially toxic elements in these oxide fractions indicated that the weathering products of pyrite and manganese pyroxene were crucial in fixing these elements, and MnO likely played an important role in controlling the behavior of heavy metals. In addition, metals were detected in significant concentrations in the exchangeable and carbonate-bound fractions, which can be toxic to the river's ecological system.

**Keywords:** tailing weathering; potentially toxic element; goethite; manganese oxide; johansennite

## 1. Introduction

Mining and subsequent processing can generate large quantities of tailings comprising sulfides and toxic elements; such tailings can cause acid mine drainage (AMD). Finely crushed mill tailings have a large surface area, rendering them particularly reactive, thereby causing elevated concentrations of potentially toxic elements in the soil and hydrological systems around the mine; sometimes, this can even affect distant areas through the river's flow [1,2]. Uncontrolled management of tailings can be a severe environmental threat including over one hundred cases of tailings dam failures recorded worldwide [3]. For example, mine tailings spilled owing to a dam rupture in 1998 in Aznalcóllar (South West Spain), wherein  $4.5 \times 10^5$  m<sup>3</sup> of acidic waters and toxic tailings spilled into the rivers, causing an adverse environmental effect on the floodplains [4–6]. Residual pollution could be detected even 20 years later, posing a continued high risk of pollution dispersion to the remaining ecosystem [7].

Over the past 40 years, approximately 1000 metal mines and 330 coal mines have been decommissioned in Korea [8]. However, the waste rocks and tailings of these mines have not been properly managed, causing severe adverse environmental impacts on the nearby soil and hydrological systems, particularly near rivers [9].

Red/brown and black/gray layers are observed at several sites along the upstream riverbank of the Nakdong River in Bonghwa, Korea. Owing to the severe weathering process caused by

river water, original mineral textures of the tailings were not observed; rather, these layers are the weathering products of the deposited tailings, washed away from the abandoned mines by past floods. The secondary minerals formed by the weathering of sulfides, such as ferrihydrite, schwertmannite, jarosite, and goethite, generally have a large surface area and high adsorption capacities, greatly reducing the mobility of the potentially toxic elements in the tailings [10–15]. Understanding the weathering process of tailings in a specific environment would thus allow the estimation of resultant mobility changes of the potentially toxic elements in that system because the tailings are vulnerable to weathering and the possibility of the leaching of these elements is high [16,17].

Effective mine waste management and restoration requires scientific knowledge of the behaviors of potentially toxic elements in that location. Various factors may affect the mobility of these elements in heavily weathered tailings located at a riverside. This work, therefore, aims to investigate the mineralogical and geochemical changes of the weathered tailings on the riverbank of the Nakdong River. This paper presents X-ray diffraction (XRD), field emission scanning electron microscopy (FE-SEM), determination of the total concentration of potentially toxic element including five-step sequential extraction data for the tailings samples, and discussing the effect of the weathering process on the behavior of these elements.

## 2. Materials and Methods

### 2.1. Sample Collection

Thirty-three samples were collected based on color, particle size, and texture of eight weathered tailings located on the riverbank of the upstream Nakdong River shown in Figure 1. Detailed descriptions of each location are listed in Table 1. Herein, eleven samples were collected from point 1; three samples were collected from point 2; four samples were collected from point 3; four samples were collected from point 4; two samples were collected from point 5; four samples were collected from point 6; two samples were collected from point 7; and three samples were collected from point 8. To preserve their original conditions as much as possible, the samples were collected using a shovel and transported to the laboratory in a plastic bag.

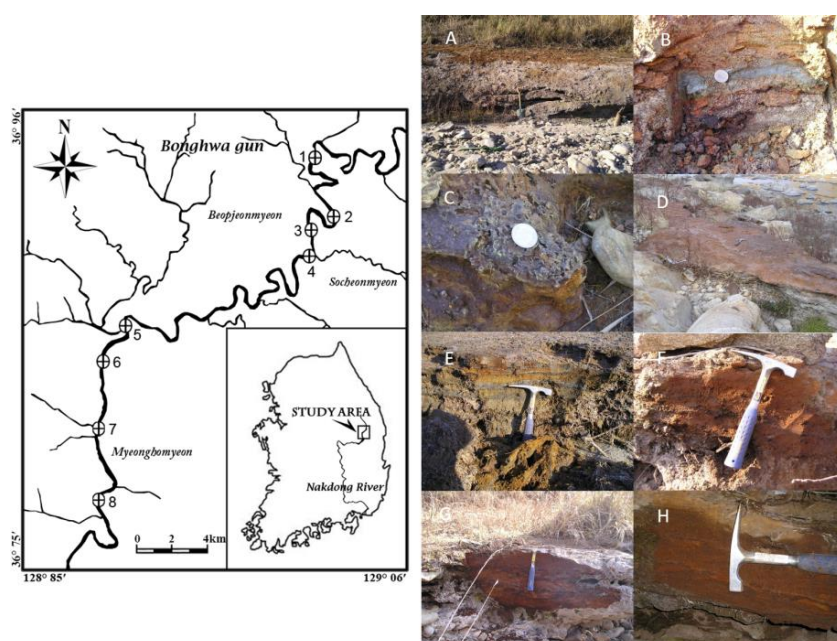


**Figure 1.** Sampling points (left) and weathered tailings layers (right) observed on the riverbank of the Nakdong River: (A,B) Point 1, (C) Point 2, (D) Point 3, (E) Point 4, (F) Point 5, (G) Point 6, and (H) Point 7.

**Table 1.** Description of each layer of weathered tailings observed on the riverbank of the Nakdong River.

Sampling Point	Number of Samples	Average Thickness	Color	pH (Average Value)
1	11	55 cm	Varied, mostly black	3.83–7.93 (6.68)
2	3	25 cm	Brown, interlayered with gray	3.22–4.05 (3.57)
3	4	45 cm	Red, gray, and black	4.15–4.87 (4.50)
4	4	15 cm	Gray, brown, black, and yellow	2.59–3.35 (3.10)
5	2	3 cm	Red with a thin black layer	6.08–6.26 (6.17)
6	4	56 cm	Red and black	4.07–5.82 (4.79)
7	2	8 cm	Brown	6.57–6.66 (6.62)
8	3	28 cm	Brown, gray, and black	6.62–6.68 (6.64)

## 2.2. Sample Analysis

The pH of each sample was measured using a pH meter (model 420A, ORION, Beverly, MA, USA) 24 h after mixing 2 g of the sample with 20 mL of deionized water with a shaker for 30 min.

To investigate their mineral compositions, the samples were dried at 60 °C for 24 h in an oven. The samples were ground using an agate mortar and analyzed via X-ray diffraction (XRD, Phillips X'pert APD, Hilversum, The Netherlands). The data were collected from  $2\theta = 5^\circ$ – $60^\circ$  with steps of  $2\theta = 0.016^\circ$  and a counting time of 1 s per step with Ni-filtered Cu-K $\alpha$  radiation at 40 KV and 30 mA at the Daegu Center of Korea Basic Science Institute. To more precisely identify secondary iron minerals, six representative samples from sampling points 1, 4, 5, 6-1, 6-2 and 7 were mixed with distilled water and dispersed using an ultrasonic cleaner for 20 min. The relatively large quartz and feldspar particles were separated using a 0.5 mm mesh sieve. The solid samples were separated via centrifugation for 5 min and then dried at 60 °C for 24 h. These samples were then analyzed via powder XRD (Bruker D5005, Billerica, MA, USA) with Fe-filtered Co-K $\alpha$  radiation at 40 kV and 30 mA at the Industrial Mineral Bank of Kangwon National University at a  $2\theta$  of  $5^\circ$ – $60^\circ$  with steps of  $0.04^\circ$  and a counting time of 8 s per step.

The morphology and texture of the primary and secondary minerals of the tailings were observed via field-emission scanning electronic microscopy (FE-SEM, Hitachi model S-4200, Hitachi, Tokyo, Japan) operating at 15 kV at the Daegu Center of the Basic Science Institute (KBSI). The chemical compositions of the minerals were additionally analyzed via energy-dispersive X-ray spectroscopy (EDS).

The concentrations of Al<sub>2</sub>O<sub>3</sub>, CaO, Fe<sub>2</sub>O<sub>3</sub>, K<sub>2</sub>O, MgO, MnO, Na<sub>2</sub>O, P<sub>2</sub>O<sub>5</sub>, SiO<sub>2</sub> and TiO<sub>2</sub> in the tailings were determined via X-ray fluorescence (XRF, Phillips PW1404, Phillips, Eindhoven, The Netherlands) operating in an ultrathin window and with a Sc–Mo X-ray tube at 4 kW at Kyungpook National University using the fused-glass method. Loss on ignition (LOI) was determined after heating the tailings to 900 °C.

The concentrations of eight potentially toxic elements (As, Cd, Co, Cr, Cu, Ni, Pb and Zn) were analyzed using the total digestion method (modified EPA3052) suggested by the Environmental Protection Agency of the United States. The samples were digested in aqua regia (HCl:HNO<sub>3</sub> = 3:1) containing HF and analyzed via an inductively coupled plasma atomic emission spectroscopy (ICP-AES, Horiba Jobin Yvon Ultima2C, Longjumeau, France) operating at 1.15 kW at a plasma gas flow rate of 12 L/min at the Seoul branch of the Korea Basic Science Institute. The spectral range was 160–800 nm with the resolution of 0.005 nm in UV. Calibration for each element confirmed that the correlation coefficient was >0.995. Sample digestion for the ICP analysis was performed using a closed-type Teflon Digestion Vessel 60 mL (Savillex, Eden Prairie, MN, USA), which is designed for rapid sample digestion via microwave or block digestion techniques. Standard samples, such as estuarine sediments

(USGS SRM 1646a) and NIST Montana Soil (NIST SRM 2711), were used to verify the analysis. The measurements of the standard samples were performed in triplicate and the mean recovery errors were within  $\pm 5\%$ . The detection limits were 0.05 ppm for As and 0.005 ppm for other elements.

The sequential extraction method modified by Li et al. [18] based on the scheme proposed by Tessier et al. [19] was used to determine the chemical fractions of the potentially toxic elements. This scheme involves five steps for each fraction: Exchangeable metals (F1), metals bound to carbonate and specially adsorbed (F2), metals bound to Fe/Mn oxides (F3), metals bound to organic matter and sulfides (F4), and metals in the residual fraction (F5). Eight elements were analyzed via ICP-AES (Jobin Yvon Ultima2C, Longjumeau, France) and ICP-mass spectroscopy (ICP-MS, Elan DRC II, Perkin Elmer, Boston, MA, USA) at 1.5 kW of radio frequency (RF) generator power with an RF frequency of 40 MHz at the Seoul branch of the Korea Basic Science Institute. The Ar nebulizer gas flow rate was 0.84 L/min. Abundance sensitivity (at  $^{23}\text{Na}$ ) was  $<1.0 \times 10^{-6}$  for the low-mass side and  $<1.0 \times 10^{-7}$  for the high-mass side. The detection limits of ICP-MS were 25 ppb for As and 2.5 ppb for other elements.

Pearson's correlation coefficient analysis was performed using SPSS (version 25.0) to correlate the concentrations of metals and pH values.

### 3. Results

#### 3.1. Sample pH

The resulting pH values ranged from approximately 3 to 8; the corresponding results are listed in Table 1. The sample with the lowest pH (3.2) was collected from point 4, whereas that with the highest pH (7.93) was collected from point 1.

#### 3.2. Mineral Compositions

The results of XRD analysis using a Cu target showed that the samples comprised quartz, feldspar, johansennite (Mn-pyroxene,  $\text{CaMnSi}_2\text{O}_6$ ), mica, amphibole, talc, and chlorite. At some sampling points, other minerals, such as gypsum (point 1), kaolinite (point 8), bassanite (point 1), and calcite (point 1) were also identified. Johansennite was primarily detected in the black samples collected from point 1.

Additional XRD analysis using a Co target was performed to identify the iron minerals of the fine particles. Goethite collected from point 6-2 and jarosite collected from point 3 were identified (Figure 2). The largest amount of johansennite was observed in the black portion of the sample collected from point 1, although it was also identified in the red/brown portions collected from other samples. Overall, the color of the samples varied with the mineral composition. The red and brown samples usually contained goethite or jarosite, whereas the black samples contained johansennite and its weathering product, manganese oxide (MnO).

SEM/EDS analysis was performed for the sample (collected from point 1-3) rich in Fe and Mn to reveal the different mineralogical features. In sample 1-3, the Fe(III) oxide and MnO coating had both smooth and irregular-shaped surfaces, as shown in Figure 3. The black sample collected from point 1-3 exhibited high concentrations of Fe and Mn: 49.7 wt% Fe and 36.67 wt% Mn, as detailed in Table 2. The Fe-containing mineral was identified as goethite via XRD. The mineral phase containing a high Mn concentration was presumed to be noncrystalline MnO because it was not identified via XRD. Therefore, goethite and MnO were the main minerals containing Fe and Mn detected in this sample. Johansennite typically has varying colors such as blue-green, gray-white, dark brown, or colorless [20]; therefore, the black color of the sample was primarily caused by Mn oxide. In the goethite and MnO, relatively high concentrations of Zn (2.82 and 17.2 wt%, respectively) and Pb (8.2 wt% in both samples) were observed (Table 2), indicating that these elements were surface-adsorbed and coprecipitated with goethite and MnO. Pb and Zn have been demonstrated to coprecipitate with iron oxide [21–23]; furthermore, Zhao et al. [24] has described the importance of the coprecipitation of Zn with MnO.

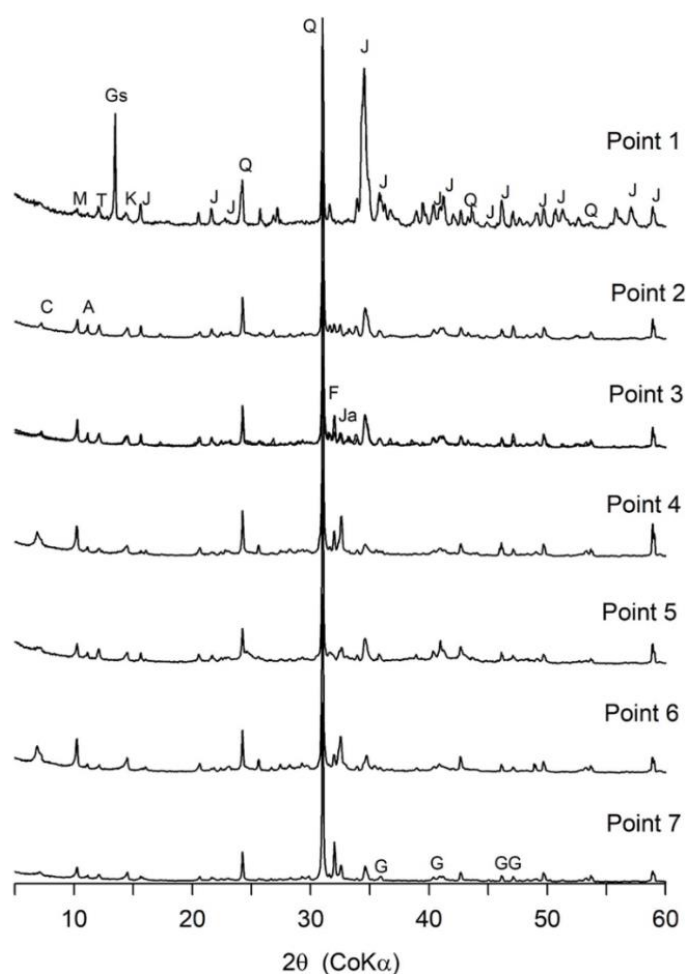


**Figure 2.** X-ray diffraction patterns of the representative weathered tailings samples with a cobalt target, where the A, C, F, G, Gs, J, K, M and T peaks represent amphibole, chlorite, feldspar, goethite, gypsum, johansennite, kaolinite, mica and talc, respectively.

**Table 2.** Chemical compositions of the samples collected from point 1-3 and 2 analyzed via EDS at each point shown in Figure 3.

B		D		E	
Element	wt%	Element	wt%	Element	wt%
O	39.29	O	36.67	O	56.80
Fe	49.72	Mn	36.04	Mg	1.10
Zn	2.82	Zn	17.21	S	16.11
Pb	8.18	As	1.82	Ca	1.95
		Pb	8.25	Mn	2.82
				Fe	22.22
Total	100		100		100

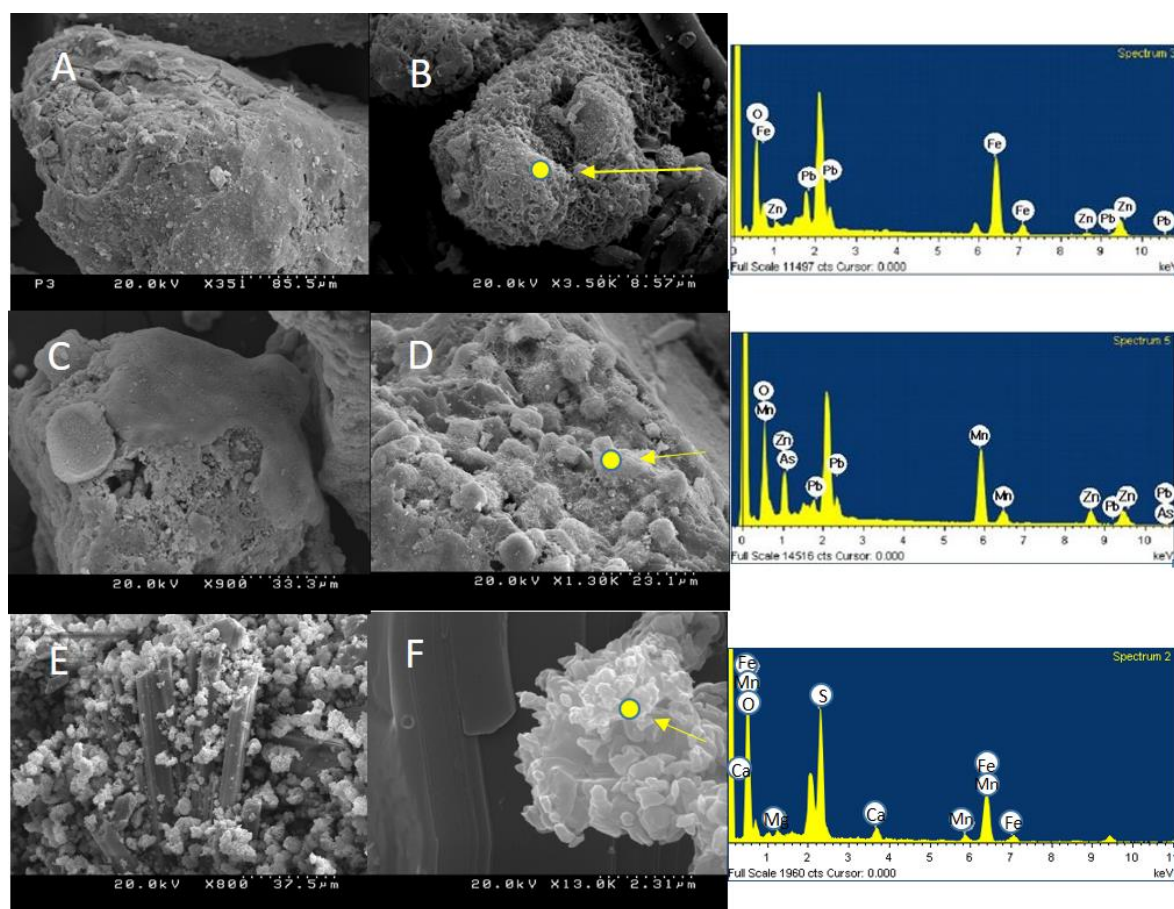


**Figure 3.** Scanning electronic microscope images and energy-dispersive X-ray spectroscopy results of the sample collected from point 1 and 2: (A) and (B): Goethite, (C) and (D): Mn oxide, (E) and (F): Schwertmannite formed on the gypsum crystal.

Minerals with fine white particles were observed in the sample collected from point 2. SEM imaging showed that these were needle-shaped gypsum particles comprising Ca and S (Figure 3). Considering the Fe, S and O composition as determined via EDS, the irregular-shaped minerals on the surface of the gypsum is likely schwertmannite ( $\text{Fe}_8\text{O}_8(\text{OH})_6\text{SO}_4$ ), which can be easily transformed to goethite [25,26].

### 3.3. Chemical Compositions of Major Elements

The chemical compositions of major elements analyzed via XRF for selected samples are listed in Table 3. Three samples were collected from point 1 to examine brown, gray, and black samples (samples 1-1, 1-2, and 1-3, respectively). The concentration of calcium was high for the samples collected from points 1 and 6, likely because of the presence of calcite in the tailings. The concentration of iron was high (3.83–7.93 wt%) for most samples owing to the weathering of pyrite. Additionally, a relatively high concentration of Mn was detected in samples collected from point 1 (4.07–5.27 wt%, as opposed to 0.74–2.28 wt% in other samples), in which johansennite and its weathering product were observed via XRD and SEM.

**Table 3.** Chemical composition of the mine tailings (wt%).

	1-1	1-2	1-3	2	3	4	5	6	7	8
Al <sub>2</sub> O <sub>3</sub>	6.84	5.79	6.37	11.16	9.42	9.26	7.13	5.94	11.43	11.4
CaO	6.52	15.28	6.28	2.31	2.85	2.55	5.67	9.74	3.58	3.94
Fe <sub>2</sub> O <sub>3</sub>	20.85	14.37	13.15	7.44	8.3	6.36	21.33	15.93	14.93	18.89
K <sub>2</sub> O	1.10	0.83	1.58	2.87	3.02	3.4	1.45	1.36	2.10	1.93
MgO	1.49	1.55	1.33	1.14	0.95	0.84	1.45	1.08	1.45	1.20
MnO	4.78	4.07	5.27	0.80	1.63	0.74	2.28	2.72	1.61	1.61
Na <sub>2</sub> O	0.37	0.22	0.55	1.31	1.19	1.45	0.56	0.61	1.34	0.97
P <sub>2</sub> O <sub>5</sub>	0.14	0.14	0.11	0.09	0.09	0.11	0.13	0.1	0.14	0.11
SiO <sub>2</sub>	50.00	38.72	57.33	64.98	67.62	71.17	51.18	48.32	54.82	49.84
TiO	0.34	0.36	0.33	0.49	0.36	0.44	0.43	0.32	0.52	0.43
LOI	7.18	18.14	7.95	7.88	5.23	3.85	9.07	13.48	8.13	9.29
Total	99.61	99.47	100.25	100.47	100.66	100.17	100.68	99.60	100.05	99.61

### 3.4. Chemical Compositions of Potentially Toxic Elements

The total concentration and mobility of eight potentially toxic elements were investigated for each weathered sample and each fraction of sequentially extracted samples. Results showed that the weathered tailings contained very high concentrations of these elements: 117.2–4,191 mg/kg of As, <5–71.29 mg/kg of Cd, <5–24.53 mg/kg of Co, 11.00–131.3 mg/kg of Cr, 20.03–173.2 mg/kg of Cu, 8,446–34,40 mg/kg of Ni, 822.49–3,720 mg/kg of Pb, and 246.3–10,996 mg/kg of Zn (Table 4). Typically, the order of potentially toxic element concentrations in the tailings samples was Zn > Pb > As > Cu > Cr > Ni > Cd > Co; in all samples, the most abundant elements were Zn, Pb, and As.

**Table 4.** Potentially toxic element concentrations of mine tailings (mg/kg).

	1-1	1-2	1-3	2	3	4	5	6	7	8
As	2178	1281	1109	117.2	132.9	499.9	4191	2303	1746	2510
Cd	15.43	18.65	71.29	11.93	7.077	<5	6.759	19.75	5.52	5.454
Co	20.38	24.53	12.29	7.432	12.39	<5	6.56	13.7	14.59	6.233
Cr	62.49	22.5	12.69	30.12	17.89	11	27.43	19.55	131.3	25.91
Cu	173.2	135.4	135.7	50.27	70.58	20.03	105.6	95.33	66.64	60.38
Ni	17.53	34.46	24.97	11.34	12.39	8.446	12.92	14.51	14.98	12.27
Pb	3270	2261	1904	208.3	836.1	82.49	1355	1481	1406	2047
Zn	5364	3201	10996	762.8	1075	246.3	1010	1567	889.8	833.1

Although the potentially toxic element concentrations provide useful information regarding the behavior of elements, different chemical forms of the elements have different potential effects on the ecosystem. Therefore, sequential extraction was performed to obtain the chemical fraction and thereby more detailed information on the toxicity of these elements. The extracted fractions of the elements in each step are shown in Figure 4 as a percentage of the sum of all fractions. The weight percentages of Cr, Ni, and Cd in the cation-exchangeable fraction (step 1) were generally larger than other elements and in the range of 0.20–42.26%, 1.58–32.28%, and 0.52–68.66%, respectively. Ni and Cr were the most predominant in the fraction of metal bound to carbonate (step 2) and were in the range of 13.57–58.92% and 15.05–39.47%, respectively. The percentages of Pb, Cr, and Zn absorbed on Fe and Mn oxides in step 3 were 25.05–89.73%, 8.84–81.85%, and 7.33–74.93%, respectively, indicating that these three elements likely coprecipitate with or strongly adsorb on Fe and Mn oxides; this is also supported by the EDS observations. The samples collected from point 1 had the highest percentage of Pb and Zn in step 3, which may be related to the high concentration of MnO. During organic or sulfide adsorption, i.e., step 4, Cu was the most predominant at 5.7–48.68%. Most of the As was found in the residual fraction, i.e., in step 5: 86.01–99.96 wt%.

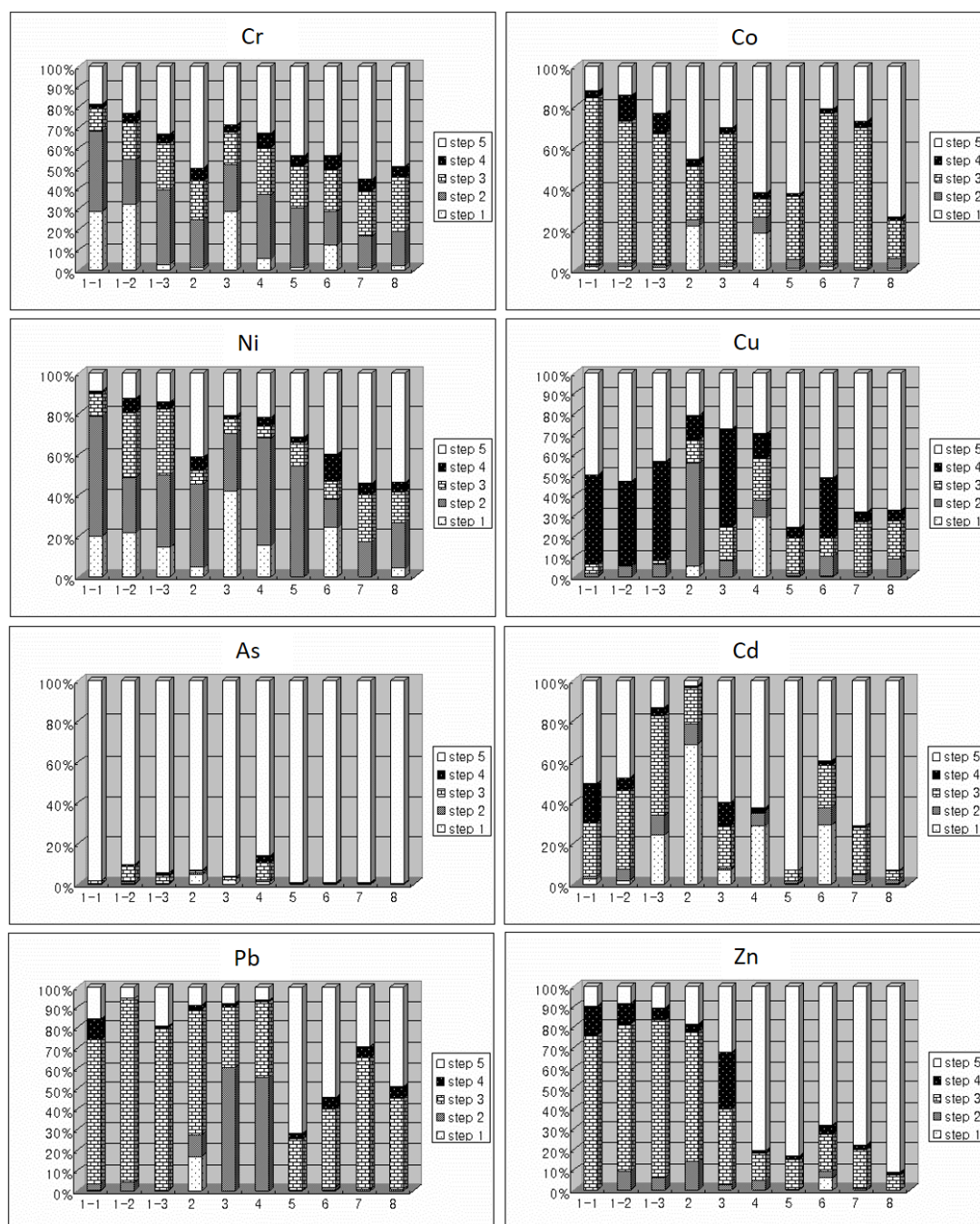


**Figure 4.** Relative abundance of the sequentially extracted potentially toxic elements for the weathered tailings samples. Step 1: Exchangeable metals, Step 2: Metals bound to carbonate and specially adsorbed, Step 3: Metals bound to Fe/Mn oxides, Step 4: Metals bound to organic matter and sulfides, Step 5: Metals in the residual fraction.

#### 4. Discussion

The various minerals identified on the tailings that had been deposited and weathered on the bank of the Nakdong River comprised primary minerals that had been moved from other places and secondary minerals that had been formed by the weathering of the tailings. The primary minerals, as observed via XRD analysis, mainly contained silicates, particularly johansennite. Secondary minerals were primarily formed during the oxidation of pyrite and weathering of silicate minerals. The elements released by the weathering of pyrite (S) and calcite and pyroxene (Ca) formed gypsum and basanite,

which are sulfate minerals. Pyrite also provided dissolved Fe for goethite formation and both dissolved Fe and S for jarosite precipitation. The K ions in jarosite can be provided by the weathering of K feldspar. MnO, which is important in fixing potentially toxic elements through coprecipitation and adsorption, directly precipitated by the weathering of johansennite. Thus, the color of the weathered tailings was mainly influenced by the weathering of pyrite and johansennite.

Schwertmannite, which is metastable and commonly found in AMD, was observed via SEM/EDS analysis and was considered to be transformed to goethite in the tailings layers. Therefore, most goethite found in the weathered tailings was probably transformed from schwertmannite. The pH, which plays an important role in the formation of iron minerals, ranged between 2.59 and 7.93. Jarosite is a common mineral in the weathered zone of sulfide ore deposits that precipitates with a high concentration of  $\text{SO}_4$  at  $\text{pH} < 3$  [14]. Jarosite was thus only observed in the sample collected from point 3, in which the pH was relatively low.

The pH values of tailings depend on the weathering of pyrite and buffering by the dissolution of calcite [27–29]. Therefore, the increase in pH observed in the samples collected from point 1 was due to the dissolution of carbonate minerals present in the mine tailings. The high concentrations of Ca detected at points 1, 5, 6, and 7 were closely related to the existence of calcite, whereas the samples collected from points 2, 3, and 4 had both a lower pH and a lower concentration of Ca. Additionally, the concentration of potentially toxic elements increased with increasing pH, showing a positive correlation with these elements and indicating that mineral compositions including pyrite and calcite were vital in controlling the behaviors of potentially toxic elements (Table 5) [28,29]. At a low pH, the mobility of these elements increases, enabling the leaching of a large portion of the elements. The samples collected from points 1, 5, 6, and 7, which had relatively high pH values and high Ca concentrations, generally showed elevated concentrations of potentially toxic elements. The correlation coefficients between the element concentration and pH for As and Cr were slightly lower than those of others, indicating that their concentrations were less correlated with pH. This is likely because they exist as oxyanions in the natural environment, unlike the other elements studied. The pH of the samples examined herein was lower than the point of zero charge of goethite and MnO; consequently, these secondary minerals have positive charges [28–31]. Therefore, As and Cr as oxyanions are dissolved less at low pH. The concentrations of As and Cr also exhibited low or negative correlation coefficients with other elements owing to their negative charges of oxyanions, compared with the high correlation coefficients among other elements.

**Table 5.** Pearson’s correlation coefficients calculated for the potentially toxic elements and pH.

	As	Cd	Co	Cr	Cu	Ni	Pb	Zn	pH
As	1								
Cd	0.130	1							
Co	0.044	0.195	1						
Cr	0.157	−0.268	0.269	1					
Cu	0.358	0.492	0.734 *	0.046	1				
Ni	0.017	0.537	0.787 **	−0.057	0.686 *	1			
Pb	0.470	0.270	0.676 *	0.220	0.860 **	0.568	1		
Zn	−0.050	0.934 **	0.366	−0.136	0.695 *	0.592	0.518	1	
pH	0.460	0.344	0.555	0.345	0.720 *	0.670 *	0.853 **	0.546	1

\*: significant at 0.05 level; \*\*: significant at 0.01 level.

SEM/EDS studies confirmed that the weathered tailings samples contained high concentrations of Pb and Zn in the Fe oxide and Zn in the MnO, particularly those collected from point 1, which generally had higher concentrations of Fe and Mn. Goethite is highly reactive and can adsorb toxic elements dissolved during weathering, and toxicity is expected to be reduced through coprecipitation and sorption [15,32]. Schwertmannite, which is supposed to precipitate first and be transformed to goethite later, also has the capacity to adsorb potentially toxic elements [13,24,26].

In many cases, potentially toxic elements can be naturally stabilized through sorption or coprecipitation with insoluble secondary minerals that are stable in an oxidizing environment such as goethite [12,15,32]. However, no detailed studies have been performed on the role of MnO in controlling these elements in natural environments. This study showed that MnO, precipitated by the weathering of Mn-pyroxene, likely plays a more important role in fixing potentially toxic elements than Fe oxide minerals.

The sequential extraction results provided more details on the mobility of each toxic element, enabling better estimation of their potential toxicity. With slight geochemical changes, the cation-exchangeable fraction (step 1) and metal fractions bound to carbonate and specially adsorbed (step 2) are more mobile, can be easily released to the water system, and are therefore, more toxic to nearby ecological systems; metals extracted in the later steps are more stable [33–36]. Cd, Cr, and Ni were present in these first two steps, albeit in low concentrations, indicating their greater potential toxicity.

Large percentages of the potentially toxic elements Co, Cd, Ni, Pb, and Zn were bound to the Fe and Mn oxides (i.e., extracted during step 3), particularly for the samples collected from point 1. As supported by the SEM/EDS analysis for Pb and Zn, these elements were supposed to be coprecipitated with or adsorbed on the surfaces of the goethite or MnO. Considering the black color and high Mn concentration of the samples from point 1, the amorphous MnO likely played a more significant role in fixing these elements; thus, weathering manganese silicate with pyrite can reduce the potential toxicity in the tailings and related systems. The most abundant potentially toxic elements in the weathered tailings were Zn, Pb, and As. Despite their elevated concentration, their potential toxicity was determined to be relatively low, as they were extracted during later steps, unlike Cd, Cr, and Ni, which, as discussed, were extracted during the first two steps. The third most abundant element, As, was mostly found in the stable residual form (i.e., extracted during step 5), providing the lowest level of toxicity in this system.

## 5. Conclusions

In this study, on an upstream riverbank of the Nakdong River, red and black layers of weathered mine tailings washed down from abandoned mines during floods were sampled and analyzed. As most ore minerals in the resulting tailings were severely weathered, the samples contained high concentrations of potentially toxic elements. The XRD analysis revealed that the samples comprised silicates, such as quartz, feldspar, mica, chlorite, amphibole, talc, kaolinite, johansennite (manganese pyroxene), and other secondary minerals, including goethite, gypsum, bassanite, and jarosite. Additionally, pyrite and calcite were identified; the pH of the samples was heavily influenced by the weathering of pyrite and buffering by the dissolution of calcite. Furthermore, the pH and the weathering of primary minerals contributed to the formation of secondary minerals. Pyrite, calcite, and johansennite were the main minerals found to influence the formation of secondary minerals. The weathering of johansennite produced amorphous MnO coated on the surface of primary minerals in black layers. Goethite was transformed from schwertmannite, which was identified via SEM analysis, and jarosite was observed in the samples with low pH values.

The overall concentrations of potentially toxic elements were in the order of Zn > Pb > As > Cu > Cr > Ni > Cd > Co. Zn, Pb and As, were the most abundant elements in all samples. Although the concentrations of Cr and Ni were relatively low, they mainly existed in cation-exchangeable forms and forms easily bound to carbonate (i.e., extracted during steps 1 and 2, respectively, of a sequential extraction method); they can, therefore, easily dissolve, causing environmental problems. Co, Cd, Ni, Pb, and Zn were more easily bound to Fe and Mn oxides (i.e., extracted during step 3), suggesting coprecipitation with and sorption on these oxides. This was particularly true in the samples collected from point 1, where the concentration of Mn was high because of the presence of johansennite and amorphous MnO. This strongly indicates that both the weathering of pyrite, producing goethite, and the weathering of johansennite are important in fixing potentially toxic elements. The third most

abundant element, As, was predominantly present in the final residue, which can be very stable even with the geochemical changes.

**Funding:** This work was supported by the National Research Foundation of Korea (NRF) grant funded by the Korean government (MSIT) (no. 2019R1A2C1002254).

**Acknowledgments:** I thank Ji-Hwan Shin for the preparation of a map and statistical analysis, and two anonymous reviewers for their constructive comments.

**Conflicts of Interest:** The authors declare no conflict of interest.

## References

1. Pagnanelli, F.; Moscardini, E.; Giuliano, V.; Toro, L. Sequential extraction of heavy metals in river sediments of an abandoned pyrite mining area: Pollution detection and affinity series. *Environ. Pollut.* **2004**, *132*, 189–201. [[CrossRef](#)] [[PubMed](#)]
2. Kossoff, D.; Hudson-Edwards, K.A.; Dubbin, W.E.; Alfredsson, M. Major and trace metal mobility during weathering of mine tailings: Implications for flood plain soils. *Appl. Geochem.* **2012**, *27*, 562–576. [[CrossRef](#)]
3. Rico, M.; Benito, G.; Salgueiro, A.R.; Díez-Herrero, A.; Pereira, H.G. Reported tailings dam failures A review of the European incidents in the worldwide context. *J. Hazard. Mater.* **2008**, *152*, 846–852. [[CrossRef](#)] [[PubMed](#)]
4. Grimalt, J.O.; Ferrer, M.; Macpherson, E. The mine tailing accident in Aznalcollar. *Sci. Total Environ.* **1999**, *242*, 3–11. [[CrossRef](#)]
5. Benito, G.; Benito-Calvo, A.; Gallart, F.; Martín-Vide, J.P.; Regües, D.; Bladé, E. Hydrological and geomorphological criteria to evaluate the dispersion risk of waste sludge generated by the Aznalcollar mine spill (SW Spain). *Environ. Geol.* **2001**, *40*, 417–428. [[CrossRef](#)]
6. Kossoff, D.; Dubbin, W.E.; Alfredsson, M.; Edwards, S.J.; Macklin, M.G.; Hudson-Edwards, K.A. Mine tailings dams: Characteristics, failure, environmental impacts, and remediation. *Appl. Geochem.* **2014**, *51*, 229–245. [[CrossRef](#)]
7. García-Carmona, M.; García-Robles, H.; Turpín Torrano, C.; Fernández Ondoño, E.; Lorite Moreno, J.; Sierra Aragón, M.; Martín Peinado, F.J. Residual pollution and vegetation distribution in amended soils 20 years after a pyrite mine tailings spill (Aznalcóllar, Spain). *Sci. Total Environ.* **2019**, *650*, 933–940. [[CrossRef](#)]
8. Ji, S.; Kim, S.; Ko, J. The status of the passive treatment systems for acid mine drainage in South Korea. *Environ. Geol.* **2008**, *55*, 1181–1194. [[CrossRef](#)]
9. Lee, J.E.; Kim, Y. A quantitative estimation of factors affecting pH changes using simple geochemical data from acid mine drainage. *Environ. Geol.* **2008**, *55*, 65–75. [[CrossRef](#)]
10. Fukushi, K.; Sato, T.; Yanase, N. Solid-solution reaction in As(V) sorption by schwertmannite. *Environ. Sci. Technol.* **2003**, *37*, 3581–3586. [[CrossRef](#)]
11. Fukushi, K.; Sato, T.; Yanase, N.; Minato, J.; Yamada, H. Arsenate sorption on schwertmannite. *Am. Mineral.* **2004**, *89*, 1728–1734. [[CrossRef](#)]
12. Burgos, W.D.; Borch, T.; Troyer, L.D.; Luan, F.; Larson, L.N.; Brown, J.F.; Lambson, J.; Shimizu, M. Schwertmannite and Fe oxides formed by biological low-pH Fe(II) oxidation versus abiotic neutralization: Impact on trace metal sequestration. *Geochim. Cosmochim. Acta* **2012**, *76*, 29–44. [[CrossRef](#)]
13. Baleeiro, A.; Fiol, S.; Otero-Fariña, A.; Antelo, J. Surface chemistry of iron oxides formed by neutralization of acidic mine waters: Removal of trace metals. *Appl. Geochem.* **2018**, *89*, 129–137. [[CrossRef](#)]
14. Kim, Y. Effects of different oxyanions in solution on the precipitation of jarosite at room temperature. *J. Hazard. Mater.* **2018**, *353*, 118–126.
15. Hajji, S.; Montes-Hernandez, G.; Sarret, G.; Tordo, A.; Morin, G.; Ona-Nguema, G.; Bureau, S.; Turki, T.; Mzoughi, N. Arsenite and chromate sequestration onto ferrihydrite, siderite and goethite nanostructured minerals: Isotherms from flow-through Reactor Experiments and XAS measurements. *J. Hazard. Mater.* **2019**, *362*, 358–367. [[CrossRef](#)]
16. Mascaro, I.; Benvenuti, B.; Corsini, F.; Costagliola, P.; Lattanzi, P.; Parrini, P.; Tanelli, G. Mine wastes at the polymetallic deposit of Fenice Capanne (southern Tuscany, Italy), Mineralogy, geochemistry, and environmental impact. *Environ. Geol.* **2001**, *41*, 417–429.

17. Meza-Figueroa, D.; Maier, R.M.; de la O-Villanueva, M.; Gómez-Alvarez, A.; Moreno-Zazueta, A.; Rivera, J.; Campillo, A.; Grandlic, C.J.; Anaya, R.; Palafox-Reyes, J. The impact of unconfined mine tailings in residential areas from a mining town in a semi-arid environment: Nacozari, Sonora, Mexico. *Chemosphere* **2009**, *77*, 140–147. [[CrossRef](#)]
18. Li, X.D.; Coles, B.J.; Ramsey, M.H.; Thornton, I. Sequential extraction of soils for multi-element analysis by ICP-AES. *Chem. Geol.* **1995**, *124*, 109–123. [[CrossRef](#)]
19. Tessier, A.; Campbell, P.G.C.; Bisson, M. Sequential extraction procedure for the speciation of particulate trace metals. *Anal. Chem.* **1979**, *51*, 844–851. [[CrossRef](#)]
20. Schaller, W.T. Johansennite, a new manganese pyroxene. *Am. Mineral.* **1938**, *23*, 575–582.
21. Martínez, C.E.; McBride, M.B. Coprecipitates of Cd, Cu, Pb and Zn in iron oxides: Solid phase transformation and metal solubility after aging and thermal treatment. *Clays Clay Miner.* **1998**, *46*, 537–545. [[CrossRef](#)]
22. Martínez, C.E.; McBride, M.B. Cd, Cu, Pb, and Zn coprecipitates in Fe oxide formed at different pH: Aging effects on metal solubility and extractability by citrate. *Environ. Toxicol. Chem.* **2001**, *20*, 122–126. [[CrossRef](#)] [[PubMed](#)]
23. Lee, G.H.; Bigham, J.M.; Faure, G. Removal of trace metals by coprecipitation with Fe, Al and Mn from natural eaters contaminated with acid mine drainage in the Bucktown mining district, Tennessee. *Appl. Geochem.* **2002**, *17*, 569–581. [[CrossRef](#)]
24. Zhao, S.; Wang, Q.; Sun, J.; Borkiewicz, O.J.; Huang, R.; Saad, E.M.; Fields, B.; Chen, S.; Zhu, M.; Tang, Y. Effect of Zn coprecipitation on the structure of layered Mn oxides. *Chem. Geol.* **2018**, *493*, 234–245. [[CrossRef](#)]
25. Jönsson, J.; Persson, P.; Sjöberg, S.; Lövgren, L. Schwertmannite precipitated from acid mine drainage: Phase transformation, sulphate release and surface properties. *Appl. Geochem.* **2005**, *20*, 179–191. [[CrossRef](#)]
26. Schroth, A.W.; Parnell, R.A. Trace metal retention through the schwertmannite to goethite transformation as observed in a field setting, Alta Mine, MT. *Appl. Geochem.* **2005**, *20*, 907–917. [[CrossRef](#)]
27. Lee, P.K.; Touray, J.C. Characteristics of a Polluted Artificial Soil located along a Motorway and Effects of Acidification on the leaching Behavior of heavy metals (Pb, Zn, Cd). *Water Res.* **1998**, *32*, 3425–3435. [[CrossRef](#)]
28. Kim, H.J.; Kim, Y.; Choo, C.O. The effect of mineralogy on the mobility of heavy metals in mine tailings: A case study in the Samsanjeil mine, Korea. *Environ. Earth Sci.* **2014**, *71*, 3429–3441. [[CrossRef](#)]
29. Park, S.; Kim, Y. Mineralogical changes and distribution of heavy metals caused by the weathering of hydrothermally altered, pyrite-rich andesite. *Environ. Earth Sci.* **2016**, *75*, 1125. [[CrossRef](#)]
30. Jurjovec, J.; Ptacek, C.J.; Blowes, D.W. Acid neutralization mechanisms and metal release in mine tailings: A laboratory column experiment. *Geochim. Cosmochim. Acta* **2002**, *66*, 1511–1523. [[CrossRef](#)]
31. Heikkinen, P.M.; Räisänen, M.L. Mineralogical and geochemical alteration of Hitura sulphide mine tailings with emphasis on nickel mobility and retention. *J. Geochem. Explor.* **2008**, *97*, 1–20. [[CrossRef](#)]
32. Jiang, W.; Lv, J.; Luo, L.; Yang, K.; Lin, Y.; Hu, F.; Zhang, J.; Zhang, S. Arsenate and cadmium co-adsorption and co-precipitation on goethite. *J. Hazard. Mater.* **2013**, *262*, 55–63. [[CrossRef](#)] [[PubMed](#)]
33. Dold, B.; Fontboté, L. A mineralogical and geochemical study of element mobility in sulfide mine tailings of Fe oxide Cu-Au deposits from the Punta del Cobre belt, northern Chile. *Chem. Geol.* **2002**, *189*, 135–163. [[CrossRef](#)]
34. Carlsson, E.; Thunberg, J.; Ohlander, B.; Holmström, H. Sequential extraction of sulfide-rich tailings remediated by the application of till cover, Kristineberg mine, northern Sweden. *Sci. Total Environ.* **2002**, *299*, 207–226. [[CrossRef](#)]
35. Caraballo, M.A.; Rotting, T.S.; Nieto, J.M.; Ayora, C. Sequential extraction and DXRD applicability to poorly crystalline Fe- and Al-phase characterization from an acid mine water passive remediation system. *Am. Mineral.* **2009**, *94*, 1029–1038. [[CrossRef](#)]
36. Kim, Y. Mineral phases and mobilities of trace metals in white precipitates found in acid mine drainage. *Chemosphere* **2015**, *119*, 803–811. [[CrossRef](#)]

